Disentangling the magnetic dimensionality of alleged magnetically isolated cuprate spin-ladder CuHpCl system. A long lasting issue.

J. Jornet-Somoza,[a,b] F. Cosi,[a] M. Fumanal,[a] M. Deumal[a]

[a] Secció Química Física, Dept. Ciència de Materials i Química Física & IQTCUB, Universitat de Barcelona, Martí i Franquès 1, E-08820, Barcelona

[b] Nano-Bio Spectroscopy Group and ETSF, Universidad del País Vasco, CFM CSIC-UPV/EHU, E-20018, San Sebastián

ABSTRACT.

The Cu_2(1,4-diazacycloheptane)$_2Cl_4$ (CuHpCl) crystal is a molecular transition metal antiferromagnetic complex, whose magnetism has been a long lasting issue. The outcome of a variety of experimental studies reported (on magnetic susceptibility, heat capacity, magnetization, spin gap and INS) provided many different *J* values depending on the fitting ladder model used. From all available experimental data, one can infer that CuHpCl is a very complex system with many competing microscopic magnetic J_{AB} interactions that lead to its overall antiferromagnetic behavior. A first-principles bottom-up study of CuHpCl is thus necessary in order to fully disentangle its magnetism. Here we incorporate data from *ab initio* computations providing the magnitude of the J_{AB} interactions to investigate the microscopic magnetic couplings in CuHpCl and, ultimately, to understand the macroscopic magnetic behavior of this crystal. Strikingly, the resulting magnetic topology can be pictured as a 3D network of interacting squared plaquette magnetic building blocks, which does not agree with the suggested ladder motif (with uniform rails) that arises from direct observation of the crystal packing. Computed magnetic susceptibility, heat capacity and magnetization data show good agreement with experiment. In spite of this agreement, it is the calculated magnetization data that enables to discriminate the different spin regimes in CuHpCl, namely gapped singlet, partially polarized and fully polarized phases. Additional analysis of the magnetic wavefunction enables to conclude that long-range spin correlation can be discarded as responsible for the partially polarized phase, whose magnetic response is in fact due to the complex interplay of the magnetic moments in the 3D magnetic topology.

Introduction.

The quest for low dimensional molecular magnets in order to study their intriguing physical properties has been a major driving force for synthetic chemists over the years. Antiferromagnetic (AFM) systems with spin gaps are a long-lasting subject of great theoretical and experimental interest. In particular, ladder systems [1] were first investigated theoretically, as toy models for high-temperature superconductivity,[2] and then experimentally.[3] We are interested in two-leg spin-½ ladders formed by two antiferromagnetically coupled Heisenberg spin chains.[1] In zero external magnetic field, their ground state is a collective singlet state (S=0), separated by a Δ gap from the first excited states which are triplets (S=1) with short ranged spin correlations.[4a] At low energies, many physical properties are dominated by the singlet-triplet Δ gap and do not depend on the underlying dynamical quantum processes stabilizing the ground state. For example, thermodynamic quantities (magnetic susceptibility, specific heat) are very similar in a number of gapped 1D Heisenberg AFM.[4b,5]

The molecular transition metal Cu_2(1,4-diazacycloheptane)$_2Cl_4$ material[6,7] (namely, $Cu_2(C_5H_{12}N_2)_2Cl_4$ or CuHpCl in short, see Figure 1a for complex formula) has been[8] (and still is[9]) the prototypical compound to quote when a magnetically isolated spin-ladder system is required due to its crystal packing consisting in well-separated ladder arrangements of copper atoms (see Figure 1c). Analysis of these ladder materials has allowed the testing of many theories of magnetic cooperative behavior, and has led to unanticipated magnetic properties, to the great interest of the magnetism community.[10] Besides being considered a prime example of a Heisenberg ladder in the strong coupling limit, the study of CuHpCl is also appealing for the reasons listed below.

Zero magnetic field as well as field-dependent properties of CuHpCl have been extensively and comprehensively studied both experimentally[4,7,8,11,12,13,14,15,16,17,18,19] and theoretically[5,20,21,22,23,24,25,26,27,28,29,30]. Therefore, our results can be fully contrasted.

CuHpCl owes its overall AFM properties to the unpaired electron formally located on the copper atoms, but actually delocalized over Cu, Cl and N atoms (see Figure 1b). Due to such unpaired electrons, the crystal could have many possible ferromagnetic (FM) or AFM microscopic J_{AB} exchange interactions between pairs of radicals resulting in the macroscopically observed magnetic behavior, which are worth exploring.

Third, the exchange energy scale is small enough[5,14b] so that by application of an external magnetic field, $H_{c1}=\Delta/g\mu_B$ ($H_{c1,exp}$ = 7.4±0.1 T), the Δ spin gap in the subsystem can be overcome, and one can drive the system through a phase transition between a gapped singlet phase and a partially polarized phase.[20a] Below H_{c1}, the magnetization remains zero (i.e. in a singlet ground state, whose first excited states are triplets.[8]).[25] Above H_{c1}, CuHpCl reaches saturation at H_{c2} ($H_{c2,exp}$ = 13.2±0.3 T), where all spins are polarized by the magnetic

field. Note that when saturation is reached, a fully polarized gapped, i.e. a FM phase is achieved. Between H_{c1} and H_{c2}, a second order phase transition appears at low temperature involving a small change in spin-entropy and no detectable change in magnetization.[4c] The spins could exhibit either a long-range ordered state or a staggered (or canted) spin structure with a uniform magnetic moment in the direction of the applied field.[4a,12,13,16b,21,28,30] Magnetization data appear to favor an ordered canted state, which is stabilized by anisotropies and 3D dipolar interactions.[8] It was suggested[4b,4d,18,21,22,23,29b,30] that this intermediate gapless phase could be regarded as a Luttinger liquid magnetic phase. [31] In such a state, there exists a quasi-long-range AFM order, and interladder exchange leads, at low enough temperature, to the formation of a Néel state.[32] Such field-induced magnetic ordering is the quasi-one-dimensional analog of a Bose-Einstein condensation (BEC) of magnons.[33] Accordingly, there are indications for CuHpCl to be considered as one of the few known realizations of BEC.[12,13a,20a,21,22,29b,34] All these data prompted us to work towards to been able to discriminate the different spin regimes in CuHpCl, namely gapped singlet, partially polarized and fully polarized phases, and to assess whether the magnetism of the intermediate gapless phase is due to long-range spin correlation or to the complex interplay of the magnetic moments in the magnetic topology.

Also, magnetically frustrated systems and systems with competing interactions are additional important areas for extensive future development. Note that here we use the physicists definition for both systems. For a system to be truly frustrated, the competing interactions must create a degenerate magnetic ground state. As mentioned, CuHpCl is considered to be a strong-rung spin ladder. It is thus one good candidate to study whether the inclusion of next-nearest-neighbor (**nnn**) interactions can introduce geometrical frustration in a 1D AFM. Quantum spin models with competing interactions represent an interesting and challenging topic for current research.[35] Such models show many unusual features in their ground state properties and are very sensitive to the approximations applied to them. It is thus exceedingly important to have strategies to handle accurately this magnetic frustration.

Summarizing, the organometallic compound CuHpCl[6,7] has been long taken as a solid representative of Heisenberg AFM S=½ ladders with both small exchange constants and spin gap (with $J_{rung} \approx 9.2$ cm^{-1}, $J_{rail} \approx 1.7$ cm^{-1} and $\Delta = 5.5 \pm 0.9$ cm^{-1}),[4,15,23,28] which makes the entire phase diagram [4b-d,12,18,19] experimentally accessible. Accordingly, all workgroups who studied CuHpCl used ladder-like models in order to fit the experimental magnetic susceptibility χ(T) data using a variety of methods.[36,37,38,39,40,41,42] The outcome of those studies provided many different fitting J values depending on the 1D model used, which were able to account for the available χ(T) magnetic response. However, it is acknowledged that fitting the magnetic data alone is not sufficient to allow the relative strengths of the parameters to be fixed extremely accurately.[8,25]

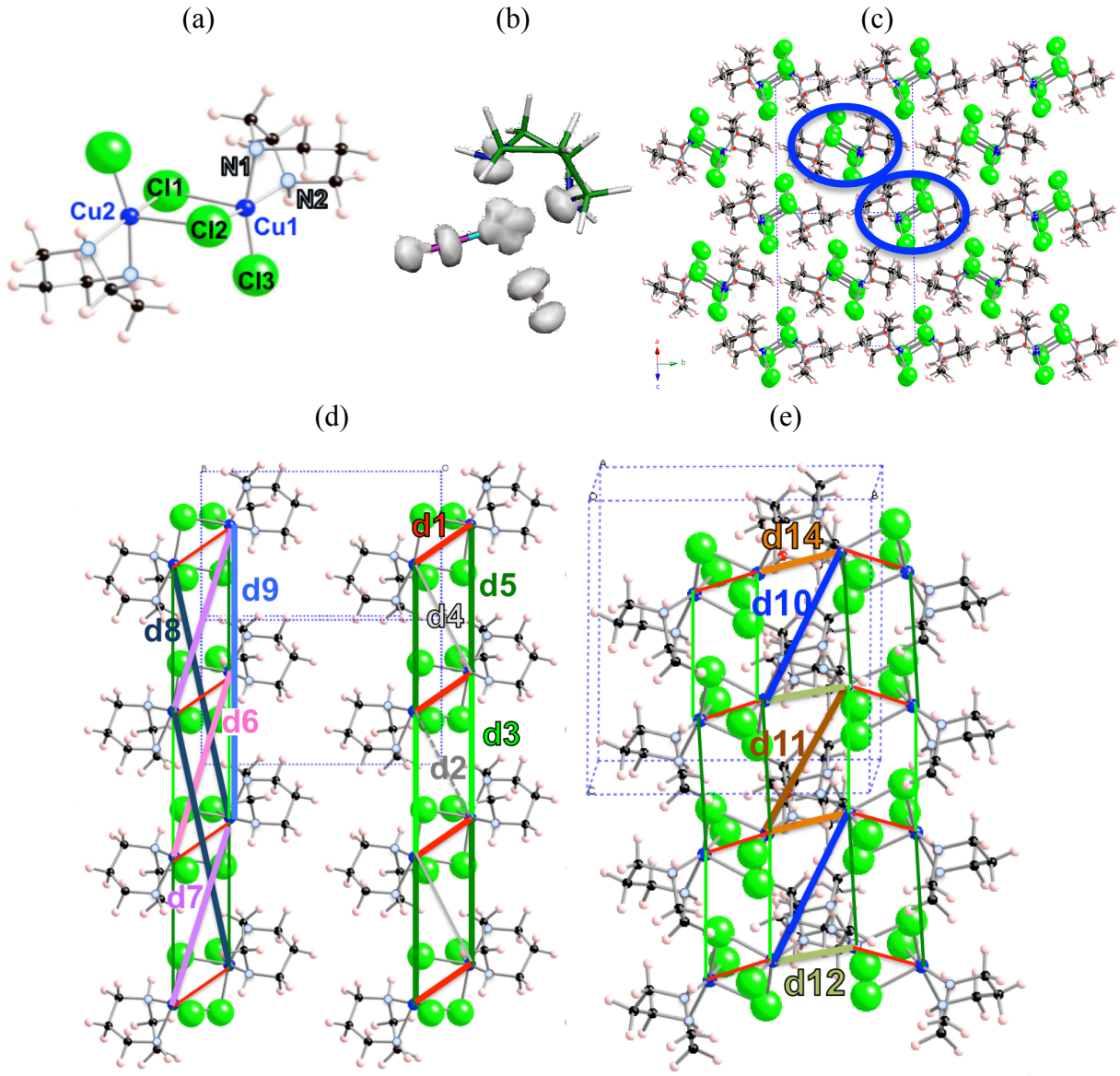

Figure 1. (a) Cu_2(1,4-diazacycloheptane)$_2Cl_4$ complex formula. (b) Spin density of $Cu(C_5H_{12}N_2)Cl_2$ monomer (isodensity surface = 0.001 au.) (c) [101] view of crystal packing of CuHpCl consisting of well-separated ladder arrangements of Cu atoms (highlighted in blue). Views of isolated ladders showing magnetically significant (d) intra-ladder pairs of radicals (first nearest neighbors **nn**: d1-d5, next-nearest neighbors **nnn**: d6-d9) and (e) inter-ladder pairs (d10-d12, d14 from spatial arrangement *A*). Connections between complex units are Cu−Cl···HN−Cu hydrogen bonding interactions. Colored lines have been added between Cu atoms to distinguish different radical···radical pairs. Color code: C (black), H (pale pink), N (light blue), Cu (blue) and Cl (green).

Magnetization M(H) is a more sensitive magnitude to magnetic dimensionality. Therefore, one should focus on M(H) in order to fully disentangle the magnetic dimensionality of CuHpCl and, in turn, reproduce and rationalize its macroscopic magnetic behavior. However, according to literature, although the techniques employed to calculate M(H) are different,[43] magnetization M(H) curves were also computed assuming that the Heisenberg spin-ladder Hamiltonian was valid.[4a,5,21,22,23,24,25,26,28,29a] Therefore, up to our knowledge, the possibility of not being an isotropic spin ladder was never given, but for one work[5] in which an alternating chain and

spin bilayer models were also considered (and ruled out after comparison to experiment). Many of the techniques described in the literature are parametric and, thus, depend on the original data by Chaboussant et al.[4] in terms of the ratio between J_{rung} and J_{leg}. Some rely upon normalizing to arbitrary values in order to be able to simulate magnetization as a function of (reduced) magnetic field (referred to as h or $h/J_{||}$ or H/Δ).[21,23,25,28] Others cannot evaluate the magnetization for low temperatures due to lack of convergence[22], or are too mathematical and the connection to chemical electronic structure information to interpret the magnetic response is harsh[20]. Altogether, the main indicator of the goodness of the method is the value of H_{c1}: the closest to the experimental 7.5 T value, the better performs the method. Accordingly, although some simulated results (which rely on experiment)[5,22] agree with the experimental H_{c1} value, others obtain different H_{c1} (for instance, 4.38T[23] using transfer-matrix renormalization group (TMRG) technique, 6.65T[5] via finite-temperature strong-coupling expansions of a spin bilayer model, and 6.8T[24] by extensive renormalization group (RG) method). To better agree with experimental data, several factors were taken into account, such as random spin impurities (which affect the H_{c2} value)[25], the diagonal J_{AB} coupling between radicals on adjacent legs (whose inclusion means that the value of J_{leg} has to be modified to keep the ratio between J_{rung} and J_{leg} constant)[25], and staggered field (Dzyaloshinskii-Moriya) terms (used as fitting coefficient)[21,28]. It must be stressed that none of them was conclusive to unveil once for all the magnetic dimensionality of CuHpCl.

The growth of larger single crystals to make a study of inelastic neutron scattering (INS) helped to lift some ambiguities about CuHpCl.[7,15b] Subsequent studies showed that the magnetic dimensionality of CuHpCl had to be more complicated than the alleged magnetically isolated spin-ladder system.[12,13,18] Therefore, however thoroughly studied, we believe that it is necessary to explicitly describe the electronic structure of the Cu-moieties within the CuHpCl crystal to unravel its magnetic topology. It is essential to identify and assess which microscopic magnetic interactions between radicals (J_{AB}) are decisive to drive the electron coupling across the crystal in order to understand its macroscopic magnetic behavior. We thus propose a bottom-up study of CuHpCl. For that purpose, the J_{AB} exchange interactions will have to be evaluated using computational quantum chemistry methods. Once evaluated, the magnetic topology of CuHpCl will be disentangled based on the magnitude of the calculated J_{AB} magnetic couplings. The relevant macroscopic magnetic response (magnetic susceptibility, heat capacity and magnetization) will then be evaluated using Statistical Mechanics by means of a First-Principles Bottom-Up (FPBU)[44] procedure, and compared to experimental data. Finally, the importance of long-range spin correlation will be assessed by analysis of the magnetic wavefunction.[45]

Computational Details

The FPBU working strategy follows four steps.[44] We use the standard static approach for both the interpretation and the simulation of its magnetic properties assuming that these properties can be obtained with a single static configuration (an X-ray resolved structure or, alternatively, an optimized structure). For CuHpCl, two crystallographically resolved structures at room temperature[6] and 4K[7] have been considered.

First, one has to select all possible magnetically relevant pairs of radicals in the crystal by analysis of the crystal packing. As for the CuHpCl crystal, the pairs of $Cu(C_5H_{12}N_2)Cl_2$ radicals have been chosen in terms of the Cu···Cu distance, taking into account that the spin density of this radical is delocalized over Cu, N and Cl atoms (see Figure 1b). Accordingly, the Cu···Cu threshold distance was set to 14.0 Å for within-ladder "di" pairs of radicals and 11.5 Å for inter-ladder "di" pairs of radicals (see Figures 1d,e and SI Section 1).

It is then next required the computation of the radical···radical J_{AB} interaction for each pair of radicals selected in the crystal. Note that hereafter the J_{AB} exchange couplings will be denoted as *J(*di*)*, where ″di″ refers to a given dimer which is identified by the distance between Cu atoms. The microscopic *J(*di*)* magnetic interaction is evaluated in terms of energy differences. Therefore, for the energy calculations, the neutral environment of any given Cu atom must be well described. Direct observation of the crystal hints at the $Cu_2(C_5H_{12}N_2)_2Cl_4$ molecular transition metal complex as the crystal packing building block (Figure 1a). We will explore which model is best to calculate the *J(*di*)* coupling for a given $Cu(C_5H_{12}N_2)Cl_2\cdots Cu(C_5H_{12}N_2)Cl_2$ pair (namely di), and whether this pair can also be taken as magnetic building block. All models explicitly evaluate the geometry of the given ″di″ pair under study, and differ on the way the environment is taken into account. Hence, the radicals directly connected to the pair were considered either (i) explicitly, (ii) replaced by point charges, or (iii) omitted (see SI Section 2). The energy calculations were performed at DFT/UB3LYP[46] level as implemented in Gaussian[47] and ORCA[48] package of programs (see SI Section 3 for benchmark against CASSCF calculations). The standard 6-31+G(d,p) basis set[49] for carbon, chlorine, hydrogen and nitrogen, and Ahlrich-pVDZ basis set[50] for copper were used in all energy calculations.

Once all intrinsic *J(*di*)* exchange couplings have been computed, one must propose the magnetic topology of the crystal in terms of the non-negligible *J(*di*)* magnetic interactions. In order to calculate the macroscopic magnetic properties of the CuHpCl crystal using Statistical Mechanics, one needs to select the minimal magnetic model space, which is the smallest set of *J(*di*)* interactions whose extension along (*a,b,c*) crystallographic axes would re-generate the entire magnetic topology.

Finally, having chosen the magnetic models, we construct the matrix representation that contains all *J(*di*)* values required to appropriately parameterize the Heisenberg Hamiltonian. Those resulting parameterized matrices are then fully diagonalized on the space of spin functions of the minimal magnetic model. The energy eigenvalues and corresponding spin numbers obtained as a result allow us to calculate the magnetic susceptibility $\chi(T)$, heat capacity $C_p(T)$ and magnetization $M(H)$ data for each magnetic model using the corresponding expression provided by Statistical Mechanics.[51] Finally the calculated data is compared to the experimentally measured data to make sure the FPBU procedure worked correctly.

Complementary to heat capacity $C_p(T)$, the magnetic capacity $C_s(T)$ will be evaluated to assess the importance of long-range spin correlation in CuHpCl,[45] since the analysis of the magnetic wavefunction enables both the study of the 3D propagation of two magnetically connected spins, i.e. short-range ordering, and magnetically non-connected spin alignment, i.e. long-range spin order/disorder. Additionally, we will monitor the temperature dependence of the magnetic correlation between all spin units to draw conclusions about the ground state of the system under consideration.

Results and Discussion

About the CuHpCl crystal: Magnetic dimensionality and basic nature of J_{AB} coupling interactions

The space group of the CuHpCl crystal is $P2_1/c$ (monoclinic, Z=4) with *a*=13.406 Å, *b*=11.454 Å, *c*=12.605 Å and *β*=115.01 for the crystal structure obtained at room temperature[6] and *a*=13.354 Å, *b*=11.246 Å, *c*=12.724 Å and *β*=115.2 for the crystal structure at 4 K[7] . As already mentioned, direct observation of the crystal packing of CuHpCl hints at a ladder like structure (Figures 1c,d). However, crystal packing and magnetic topology do often not agree. The calculation of the value of the microscopic exchange *J(*di*)* interaction between radicals requires the choice of the most adequate cluster model. It is important to realize that the CuHpCl complex is formed by two $Cu(C_5H_{12}N_2)Cl_2$ units bridged by two chlorines atoms (see Figure 1a). Although those two $Cu(C_5H_{12}N_2)Cl_2$ units are not directly related by a crystallographic inversion center, the coordination environment around the two copper atoms is very similar, and $Cu_2(C_5H_{12}N_2)_2Cl_4$ can be regarded as a centrosymmetric binuclear molecular unit. Each metal center Cu1 shows a distorted square pyramidal coordination: Cu1 establishes four short bonds with two nitrogen atoms (N1&N2) of the 1,4-diazacycloheptane ligand, a terminal chlorine atom (Cl3), and a bridging chlorine atom (Cl2) (as shown on Figure 1a). The long, apical bond involves a basal chlorine atom (Cl1) of the other copper atom (Cu2). The presence of two bridged copper atoms indicates that the magnetic unit may not be correctly described within a monomeric model, but considering the dimer as a non-

separable biradical specie. One then should notice that $Cu_2(C_5H_{12}N_2)_2Cl_4$ are connected into infinite ladder-like chains (see Figure 1d). The ladder motif is found to present two types of radicals forming the rails depending on the Cu···Cu distance being: (i) 6.996 Å with 5.774 Å and 9.380 Å distances between the radicals forming the two diagonals (d3, d2 and d7, respectively, in Figure 1d), and (ii) 7.002 Å with diagonal 5.822 Å and 9.358 Å distances (d5, d4 and d7, respectively, in Figure 1d). For both cases, the rung, formed by the two coppers of the $Cu_2(C_5H_{12}N_2)_2Cl_4$ unit (see Figure 1a), has a unique Cu···Cu distance of 3.422 Å (d1 in Figure 1d). The equivalent distances obtained at 4K[7] are slightly shorter at lower temperatures due to thermal contraction (see Table 1 and SI Section 1). However, no significant differences are observed.

Overall, nine different within-ladder pairs of radicals were selected according to the 14Å threshold (see Table 1 for Cu···Cu distances using crystal data determined at T_{room} and 4 K). Among them, there are five d1-d5 nearest neighbors (**nn**), and four d6-d9 next-nearest neighbors (**nnn**) radical pairs, respectively (see Figure 1d and SI Section 1 for illustration of all selected d1-d9 radical pairs).

Previous studies published about CuHpCl molecular magnet assumed that ladders were connected through van der Waals forces.[4a] As a result of this hypothesis, the microscopic magnetic exchange between ladders was neglected. In order to check whether they are magnetically isolated or not, we also selected fifteen pairs of radicals arising from four *A*-*D* different spatial arrangements between ladders (see discussion in SI Section 1). Note that all selected d10-d24 radical pairs are classified in terms of Cu···Cu distances. Dimers from the first spatial arrangement *A* are schematically illustrated in Figure 1e (see Table 1 for Cu···Cu distances using crystal data determined at T_{room} and 4 K).

Table 1. Cu···Cu distances at the crystal structures resolved at room temperature T_{room} and 4 K (in Å) of selected within-ladder radical pairs (**nn** stands for nearest-neighbor and **nnn** for next-nearest neighbor radicals in Figure 1d) and between two nearby spin-ladders radical pairs (spatial arrangement *A* identified in the CuHpCl crystal in Figure 1e). See SI Section 1 for spatial arrangements *B*-*D*.

Cu···Cu distance within-ladder (intra-ladder) /Å **nn** pairs				Cu···Cu distance within-ladder (intra-ladder) /Å **nnn** pairs			Cu···Cu distance between ladders (inter-ladder-*A*) /Å		
di	T_{room}	4 K		di	T_{room}	4 K	di	T_{room}	4 K
d1	3.422	3.376		d6	9.358	9.328	d10	6.998	7.026
d2	5.774	5.757		d7	9.380	9.344	d11	7.033	7.059
d3	6.996	6.987		d8	12.380	12.344	d12	7.206	7.156
d4	5.822	5.814		d9	13.990	13.987	d14	7.552	7.504
d5	7.002	7.000							

Therefore, after the analysis of the crystal packing, twenty-four pairs of radicals were selected. Accordingly, the magnetism of the CuHpCl crystal might be due to through-bond (d1) as well as through-space (d2-d24) microscopic pair interactions between $Cu(C_5H_{12}N_2)Cl_2$ radicals. The next step in our work strategy is to compute the *J(*di*)* microscopic interaction between pairs of radicals in order to discriminate which pair will contribute to the magnetic topology of the crystal.

Previous experience on *J(*di*)* models[52] and observation of the crystal packing hint that the very near disposition of the monomers in the closest through-bond d1 dimer, which includes two shared Cl atoms (see Figure 1a), will possibly lead to a poor Madelung field description for a quantitative *J(*di*)* calculation using the simplest dimer approach for pair interactions other than d1. Therefore, in order to rule out possible problems related to a dimeric cluster model, both intra- and inter-ladder *J*(di) interactions have been computed using a 4-radical tetramer model that always considers the dimer d1 unit as a non-separable magnetic moiety (for instance, see Figure 2a for tetramer model to calculate *J*(d3) and SI Section 2 for further discussion on choice of model). Let us mention here that we considered *J*(di) values smaller than $|0.1|$ cm^{-1} as negligible due to the accuracy of our calculations.[53]

According to Table 2, the magnetic topology is actually different from a spin-ladder motif (see Figure 2b) since only AFM *J*(d5) and FM *J*(d1) are magnetically relevant (note that *J*(d3) is one order of magnitude smaller). Therefore, the magnetic topology can be pictured as squared plaquettes formed by AFM *J(*d5*)* (in green) and FM *J(*d1*)* (in red) (and diagonal *J(*d6*)* in light blue) connected via *J(*d12*)* (in orange) and *J(*d14*)* (in yellow) in an AFM 2D shape along the *ab*-layer, that pile up antiferromagnetically along *c* to give rise to a 3D magnetic topology. This magnetic picture is preserved at both room temperature and 4 K since no significant differences are observed in the values of the *J(*di*)* coupling interactions. This can be attributed to the fact that, although radicals stack along the *c*-axis (see Figures 1c-e), their crystal packing avoids a π-π overlap of radicals.[54] Note that spatial arrangements *B*-*D* do not provide magnetically active radical pairs (SI Section 1).

To sum up, the resulting magnetic topology presents a clear competition of FM and AFM *J(*di*)* magnetic channels. However, the spin arrangement shows no geometrical frustration, i.e. the disposition of the FM *J(*d1*)* coupled radicals is compatible with all three remaining AFM *J(*di*)* intra- and inter-plaquette couplings (see Figure 2c for a schematic representation). The inter-plaquette interactions (so-called inter-ladder in Table 2) are revealed to be magnetically significant, contrary to common believe.[4a-b,22] Therefore, the 3D magnetic topology has indeed proved to be more complex than expected from direct observation of the crystal packing, as hinted from INS[7,15b] and NMR[18] experiments.

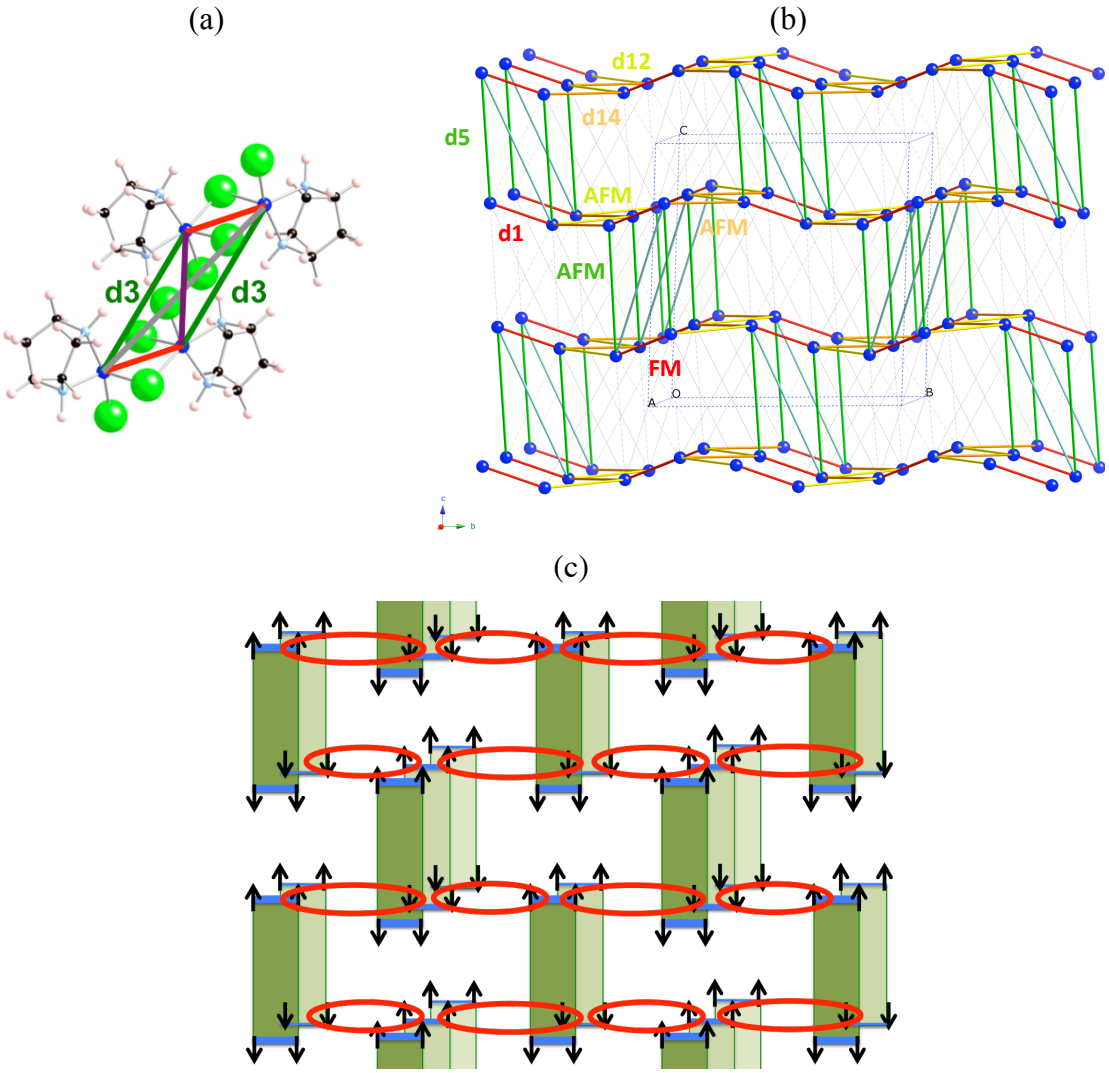

Figure 2. (a) Evaluation of *J(d3)* (in green) using as a cluster model a tetramer (namely d1 in red, d2 in grey & d7 in purple). (b) Magnetic topology of CuHpCl, where only copper atoms are represented. Color code: intra-plaquette AFM *J(*d5*)* green, FM *J(*d1*)* red, and diagonal AFM *J(*d6*)* light blue ; inter-plaquettes AFM *J(*d12*)* orange and AFM *J(*d14*)* yellow. Dashed lines for $|J(\text{di})| < 0.1$ cm^{-1}. (c) Possible spin arrangement in agreement with the magnetic topology of CuHpCl showing FM and AFM *J(*di*)* competition (intra- and inter-plaquettes) but no geometrical frustration.

Table 2. Magnetically non-negligible *J*(di) interactions (in cm^{-1}) of selected radical pairs. Results using tetramer cluster models for both intra- and inter-ladder *J(*di*)* are shown for the room temperature (T_{room}, HT) and 4K (LT) crystal structures.

		intra-ladder					***inter-ladder***			
		--------- nn ---------				***---- nnn ----***				
model	T	***J*(d1)**	***J*(d3)**	***J*(d5)**	***J*(d6)**	***J*(d7)**	***J*(d10)**	***J*(d11)**	***J*(d12)**	***J*(d14)**
tetramer	T_{room}	+2.37[a]	-0.13	-3.58	-0.29	-0.13	+0.33	-0.11	-1.01	-1.19
	4 K	+2.30[a]	-0.37	-3.88	-0.29	-0.12	+0.22	-0.31	-1.05	-1.38

[a] Average value using *J*(d1*)* resulting from the calculations to obtain *J(*d3*)* and *J(*d5*)* using a tetramer.

Table 3. Comparison between atomic charges and spin densities for d3 and d5 pairs of radicals. Atomic charges and spin densities have been computed using the CM5[55a] and Hirshfeld[55b,c] approaches, respectively. Note that the atom numbering is explicitly given in the figure inset, which displays the two Cl···H-N magnetic channels present in both d3 and d5 dimers. Color code: Cl in light green, H in light pink, N in light blue, Cu in blue, C in black.

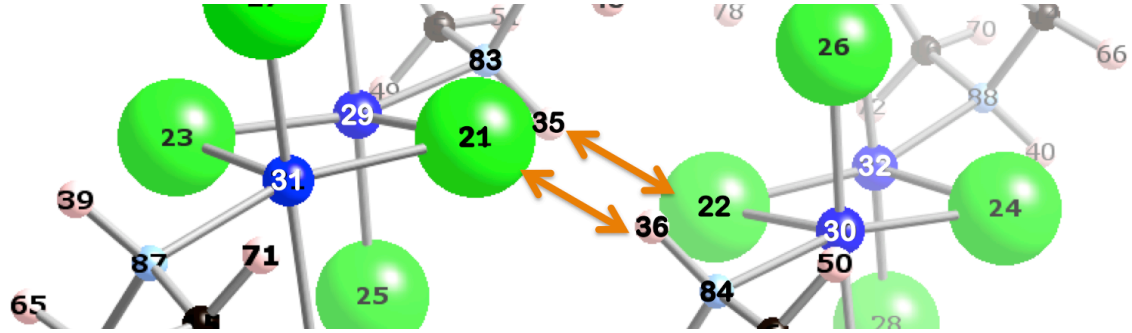

§	Cu31	Cu29	Cl21		H36	N84		Cu30	Cu32
atomic charges									
d3	0.4702	0.4707	-0.3013		+0.2908	-0.5566		0.4706	0.4698
d5	0.4675	0.4735	-0.2877		+0.2898	-0.5515		0.4738	0.4678
spin density									
d3	0.5733	0.5733	0.084		0.0044	0.0955		0.5733	0.5791
d5	0.5718	0.5808	0.090		0.0049	0.1007		0.5808	0.5718

§ Channels Cl21···H36-N84 and N83-H35···Cl22 are equivalent.

Further, it is interesting to pay attention to the fact that J(d3) and J(d5) have remarkably different magnitude but a very similar geometry (see Figure 1d). This apparent similarity does not hold when analyzing the atomic charges[55a] of the Cl···H-N atoms involved in channeling the magnetic coupling for d3 and d5 (namely, Cl21···H36-N84 and Cl22···H35-N83 in figure inset in Table 3). According to Table 3, it is possible to observe that there is a larger charge polarization of the atoms channeling the magnetic interaction for d3 than for d5, which can be taken as a signature for a larger degree of hydrogen bonding in d3. The fact that hydrogen bonding enhances FM exchange coupling between radicals has previously been encountered and documented.[56] Note that the hydrogen bonding qualitative argument is based on the fact that it is assumed that the more polarized the hydrogen atoms are (i.e. the larger their partial positive charge is), the stronger the bond is (see discussion in SI Section 4). It follows that a less AFM J_{AB} value should be thus expected for radical pairs with a larger contribution from hydrogen bonding (J(d3) = -0.37 cm^{-1} vs. J(d5) = -3.88 cm^{-1}). In addition, we have also analyzed the spin density[55b,c] along the Cu-Cl···H-N-Cu path which couples $Cu(C_5H_{12}N_2)Cl_2$ radicals (see Table 3). Note that H36 of d3, which carries the largest partial charge, has smaller spin density than H36 of d5, as expected since hydrogen bonding in d3 is stronger than in d5. In addition, according to calculations, the spin density is larger in d5, which leads to a stronger AFM interaction.

Computing magnetic properties: $\chi(T)$, $C_p(T)$ and $M(H)$

Analysis of the magnetic topology of CuHpCl (Figure 2b) reveals that the magnetic building block is a 4-radical plaquette consisting in two binuclear ferromagnetic d1 moieties interacting antiferromagnetically by means of d5. The magnetic models contemplated must consider both isolated tetramer magnetic building blocks as well as 3D magnetic models consisting of plaquettes interacting through AFM *J(*d12*)* and *J(*d14*)* couplings (see SI Section 5). The magnetic response of CuHpCl (namely, magnetic susceptibility $\chi(T)$, heat capacity $C_p(T)$ and magnetization $M(H)$) has been simulated considering the *J(di)* values from the 4 K crystal structure[7] obtained by means of the tetramer approach at DFT/UB3LYP level. Note that the gyromagnetic factor *g* is set to be 2.08.[4a]

Comparison of calculated $\chi(T)$ curve with the experimental measurements (black[11b] in Figure 3a) shows good agreement, when the magnetic model used enable squared plaquette magnetic building blocks interact through AFM inter-plaquette interactions. The situation of the χ peak is at *ca.* 7 K, and its intensity is about 0.030 emu mol^{-1}, just 0.007 emu mol^{-1} far from the experimental 0.023 emu mol^{-1} value. The same calculation has been done with the crystal structure obtained at room temperature.[6] As the magnetic topology is hardly affected by the temperature, i.e. the magnitude of the magnetic exchange values is only slightly influenced by thermal contraction (Table 2), a re-calculation of the $\chi(T)$ curve shows no significant differences with respect to the calculations performed using the coupling values at 4 K (see SI Section 5 for a full discussion). Note that the calculated and experimental magnetic susceptibility data perfectly agree above 60 K.

Calculated heat capacity $C_p(T)$ data also agree with the available experimental data (see Figure 3b). Both calculated and experimental $C_p(T)$ curves have the same shape and their intensities are almost identical (namely, the computed heat capacity shows a peak at temperature about 4.0 K, which is consistent with the experimental peak at 4.6 K), irrespective of the magnetic model.

It follows that magnetic susceptibility and heat capacity data for CuHpCl are little sensitive to magnetic dimensionality, as has been already pointed out by experimentalists.[5] This is the reason why a large variety of fitting models performed in good agreement with experiment,[4a,5,6,15] although those models did not represent the magnetic topology of CuHpCl. Contrarily, magnetization data is more sensitive to magnetic models, and it thus will provide more sound information about the dimensionality of the system under study (see SI Section 6 for an illustration of the sensitivity of calculated *M(H)* data on the magnetic model). Therefore, hereafter we will focus on reproducing the magnetization *M(H)* data of CuHpCl. Note we have used the reduced definition of magnetic field to compare our results to the experimental magnetization data, in line with Refs. [23,25].

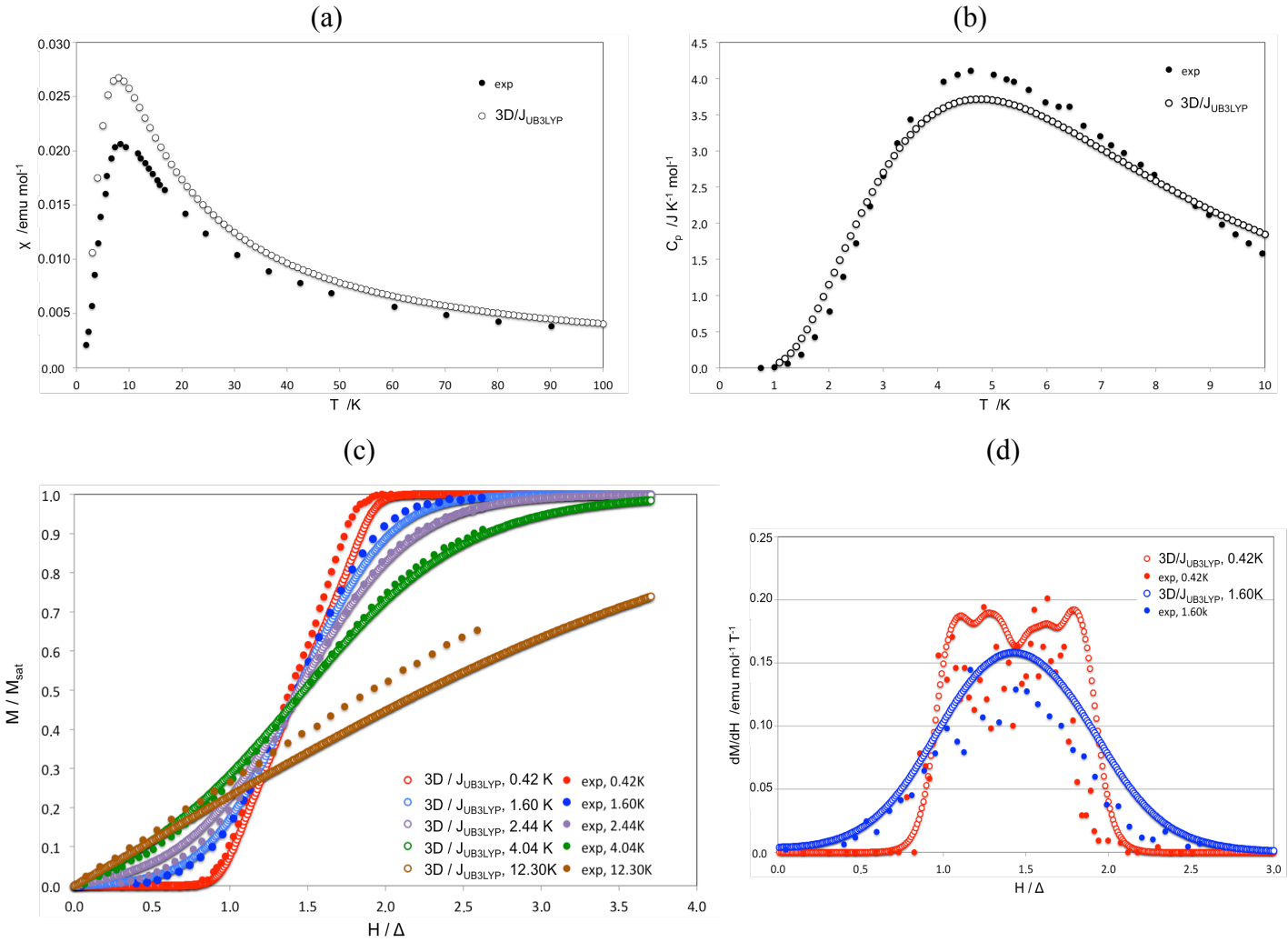

Figure 3. Comparison between experimental data (filled symbols) and calculated data (empty symbols) using the J_{AB} values obtained by the tetramer approach at 4 K to define a minimal 3D magnetic model for (a) magnetic susceptibility $\chi(T)$, (b) heat capacity $C_p(T)$, (c) magnetization M/M_{sat} as a function of the H/Δ reduced magnetic field, and (d) dM/dH(H/Δ). See Figure S5.2b in SI Section 5 for minimal 3D magnetic model. Experimental Δ value is $H_{c1,exp}$ 7.4 T. See inset (c,d) for color code referring to simulation temperature.

From the lowest temperature $M(H)$ curve at 0.42 K (Figures 3c,d in red), our data agree with a nonmagnetic solid below 5.2 T, whose magnetization remains zero. Below H_{c1}, a singlet ground state separated from S≠0 excitations is thus observed, and CuHpCl apparently behaves as a commensurate or gapped phase that has 3D long range ordering due to inter-plaquette couplings. Boltzmann population corroborates that the ground state is a singlet and there are accessible triplet states (see Table S7.1 in SI Section 7). At this point, one can obtain the spin gap (Δ_{gap}) as the energy difference between the singlet ground state and the first triplet state, which is provided by solving the Heisenberg secular equation problem in the space defined by the minimal 3D magnetic model. The resulting Δ_{gap} is found to be 5.4 cm^{-1}, which is in agreement with the experimental singlet and triplet spin-gap value provided by the literature (namely, 7.5[4a], 4.7 and 6.4[15a] cm^{-1}). Note that the Δ_{gap} extracted from the eigenvalues

of the full diagonalization of the corresponding Heisenberg hamiltonian results in a 5.5 T critical field ($H_{c1} = \Delta_{gap}/g\mu_B$), which indirectly supports our estimated value of 5.2 T for H_{c1}.

Further observation of $M(H)$ at 0.42 K shows that, with increasing field, the magnetization increases until it reaches its saturation value at 10.4 T, above which CuHpCl is fully FM polarized (Figures 3c,d in red). The intermediate partially polarized phase is revealed between H_{c1} and H_{c2}. The magnetization data has been further simulated at different temperatures ranging from 1.60K to 12.30K for which there is available experimental data. Comparison between calculated and experimental data is remarkable (see empty vs. filled symbols, respectively, in Figure 3c). As temperature increases, the different spin regimes eventually cannot be realized because at very low magnetic field not only the ground state singlet but also many other higher multiplicity states are populated (see Table S7.1 in SI Section 7) and, in turn, CuHpCl cannot behave any longer as a non magnetic solid since magnetization is different from zero. Note that the critical fields H_{c1} and H_{c2} are better estimated from the representation of dM/dH as a function of the reduced magnetic field (see Figure 3d for comparison between data at 0.42K and 1.60K). We must highlight that, although the magnetic topology was hardly affected by the temperature (i.e. the magnitude of J_{AB} magnetic exchange values were only slightly influenced by thermal contraction), the calculated H_{c1} and H_{c2} values have a non-negligible dependence on the temperature at which the crystal structure of CuHpCl has been characterized (see discussion in SI Section 6). Unexpectedly, using calculated data at RT, H_{c1} is *ca.* 4.7 T, at 4 K is *ca.* 5.2 T and at 0.42 K (experimental) 7.4 T. The magnetic field range spanning between H_{c1} and H_{c2} is also temperature dependent. If lower than 4 K crystal data was available, no doubt our estimated value of H_{c1} would be further improved. Also, in view of the high sensibility of H_{c1}, thermal fluctuations might play a role in fine tuning the estimated value of H_{c1}. Note that the inclusion of thermal fluctuations is done by means of *ab initio* molecular dynamics (AIMD), which are out of the scope of this paper. Therefore, the crystallographic data plays a non-innocent role in determining the values of the critical field. Having clarified this issue, now we are left with the analysis of the magnetic wavefunction[45] of CuHpCl to provide a deeper insight into the origin of the behavior of the intermediate partially polarized phase.

Let us finally draw attention to our recently proposed descriptor of the magnetic topology, the magnetic capacity $C_s(T)$,[45] since it is a measure of the thermal variation of the spin multiplicity of the system and reflects the importance of magnetically non-connected spin alignment and how the dominant effect of long-range spin correlation governs the magnetic behavior of molecule-based crystals (and in general of magnetic compounds). In the same study it was also concluded that $C_p(T)$ measures the energy variation due to the 3D propagation of the interaction of two magnetically connected spins, that is, to short-range ordering. Therefore, analyzing the behavior of the critical temperature T_C of both magnetic

$C_s(T)$ and heat $C_p(T)$ capacities provides information on the importance of long-range spin correlation. For CuHpCl, we discover that T_C calculated from either $C_p(T)$ or $C_s(T)$ is nearly identical (see SI Section 7). We know this is the case only in those molecule-based systems in which either the long-range spin correlation can be neglected, or there is no 3D propagation of the spin coupling. Since we have determined that the magnetic topology is 3D, we must conclude that the long-range spin correlation can be neglected. This is in fact corroborated by the analysis of the magnetic wavefunction at different temperatures (see also SI Section 7), which shows little contribution of long-range spin correlation as already appraised (even at very low temperature). It thus follows that the long-range spin correlation can be discarded as responsible for the partially polarized phase, which is in fact due to the complex interplay of the magnetic moments in the 3D magnetic topology of CuHpCl.

Conclusions

We have studied the magnetism of the Cu_2(1,4-diazacycloheptane)$_2Cl_4$ crystal, namely CuHpCl, at 4 K and at room temperature using a first principles bottom-up procedure. It has been found that the standard dimer model is here of no use to evaluate *J(*di*)* interactions between pairs of radicals since there is a magnetic $Cu(C_5H_{12}N_2)Cl_2\cdots Cu(C_5H_{12}N_2)Cl_2$ moiety that behaves as a biradical and cannot be split in two. Instead, an extended tetramer cluster model is needed to obtain quantitative results for all magnetic *J(*di*)* radical pair interactions. Hydrogen bonding formation has been found to be determinant to enhance ferromagnetic interactions and, in turn, reduce (in absolute value) the magnitude of *J(*di*)* AFM couplings. In addition, *J(*di*)*'s have been found to be very little affected by the thermal compression, mainly because radicals of CuHpCl do not pile up forming π–stacks in the crystal packing.

The magnetic topology of CuHpCl results from the competition among nine microscopic magnetic *J(*di*)* pair exchange interactions. Our results agree with a cooperative network of ferromagnetic units coupled antiferromagnetically giving rise to squared plaquette magnetic building blocks, which are then antiferromagnetically connected: first in a 2D motif along the *ab*-layer, and next piling up along *c* to give rise to the 3D overall magnetic topology. The spin arrangement shows no geometrical frustration. Accordingly, the resulting 3D magnetic topology agrees with reported INS/NMR experiments[7,12,15,18] on CuHpCl that predicted a 3D transition at low temperatures, i.e. hinted at the magnetic dimensionality to be more complicated than that of an AFM spin-ladder system. In this sense, our work clearly calls into question the validity of the alleged magnetically isolated ladder motif (with uniform rails) arising from direct observation of the crystal packing and from fitting the experimental magnetic susceptibility data to a parametric ladder model.

The computed $\chi(T)$, $C_p(T)$ data and singlet and triplet spin gap fit properly the experimental data. The temperature at which $\chi(T)$ is maximum is well reproduced (7K vs. experimental 8K) and, from the maximum of $C_p(T)$ data, one can infer the critical temperature to be about 4.6K (experimentally 4.0K). Interestingly, magnetization $M(H)$ data is found to be more sensitive to magnetic models than $\chi(T)$ and $C_p(T)$. Therefore, using the most appropriate 3D magnetic model, $M(H)$ provides sound information about the magnetic dimensionality and magnetic regimes (gapped singlet, partially polarized and fully polarized) of CuHpCl. The analysis of the Boltzmann population of the magnetic wavefunction enables to assess which states are populated and, thus, contribute to the magnetic response. Finally, by monitoring the temperature dependence of the magnetic correlation between all spin units, it has also been concluded that long-range spin correlation can be discarded as the origin of the partially polarized phase of CuHpCl, which actually results from the complex interplay of the magnetic moments in the 3D magnetic topology.

Within the framework of molecule-based magnetism, the first-principles bottom-up computational study of CuHpCl aims at capturing the microscopic complexity of the molecular material to both attain an adequate understanding and reproduce the available experimental magnetic data. In contrast to other strategies that do not explicitly account for the electronic structure of the material and simply aim at fitting the experimental magnetic data to a parametric model that might (or not) resemble the crystal packing, computational chemistry can provide a sound insight into the nature and mechanism of the magnetic coupling. Therefore, the information furnished by quantum chemistry is exceedingly important in the Materials Science community since it can be envisaged as an exploratory tool for the design of new and complex multifunctional materials.

Conflicts of interest

There are no conflicts to declare.

Acknowledgements

MD acknowledges financial support from MINECO (projects MAT2014-54025-P and CTQ2017-87773-P/AEI/FEDER, UE), Spanish Structures Excellence María de Maeztu program (MDM-2017-0767), and Catalan DURSI (2014-SGR-1422 and 2017SGR348).

Supporting information (SI). Section 1: Geometry of d1-d24 radical pairs with Cu···Cu distance at 4 K and room temperature. Inter-ladder d10-d24 dimers are displayed according

to *A*-*D* spatial arrangements. **Section 2:** Tetramer model to calculate *J*(di). **Section 3:** Benchmark of UDFT against CASSCF calculations for *J*(d3) and *J*(d5). **Section 4:** *J*(d3) vs. *J*(d5). **Section 5:** Magnetic models used to calculate magnetic susceptibility $\chi(T)$. Sensitivity of M(H) data vs. magnetic model. **Section 6:** Experimental vs. calculated magnetization *M(H)* data. **Section 7:** Heat C_p(T) and magnetic C_s(T) capacities. Analysis of the magnetic wavefunction.

References

[1] For a review: (a) E. Dagotto and T.M. Rice, *Science*, 1996, **271**, 618. (b) E. Dagotto, *Rep. Prog. Phys.*, 1999, **62**, 1525

[2] T.M. Rice, S. Gopalan, and M. Sigrist, *Europhys. Lett.*, 1993, **23**, 445.

[3] M. Azuma, Z. Hiroi, M. Takano, K. Ishida, and Y. Kitaoka, *Phys. Rev. Lett.*, 1994, **73**, 3463.

[4] (a) G. Chaboussant, M.-H. Julien, Y. Fagot-Revurat, M. Hanson, L.P. Lévy, C. Berthier, M. Horvatic, and O. Piovesana, *Eur. Phys. J. B*, 1998, **6**, 167. (b) G. Chaboussant, M.-H. Julien, Y. Fagot-Revurat, L. P. Levy, C. Berthier, M. Horvatic, and O. Piovesana, *Phys. Rev. Lett.*, 1997, **79**, 925. (c) G. Chaboussant, Y. Fagot-Revurat, M.-H. Julien, M.E. Hanson, C. Berthier, M. Horvatic, L. P. Levy, and O. Piovesana, *Phys. Rev. Lett.*, 1998, **80**, 2713. (d) G. Chaboussant, M.-H. Julien, Y. Fagot-Revurat, H. Mayaffre, M. Horvatic, L.P. Levy, C. Berthier, and O. Piovesana, *Physica B*, 2000, **280**, 315. (e) G. Chaboussant, *Contribution de la diffusion des neutrons à l'étude des aimants moléculaires,* Habilitation Dissertation, Université Pierre et Marie Curie - Paris VI, Paris, 2009.

[5] N. Elstner, and R.R.P. Singh, *Phys. Rev. B*, 1998, **58**, 11484

[6] B. Chiari, O. Piovesana, T. Tarantelli, and P.F. Zanazzi, *Inorg. Chem.*, 1990, **29**, 1172

[7] M.B. Stone, Y. Chen, J. Rittner, H. Yardimci, D.H. Reich, C. Broholm, D.V. Ferraris, and T. Lectka, *Phys. Rev. B*, 2002, **65**, 64423

[8] G. Chaboussant, P.A. Crowell, L.P. Levy, O. Piovesana, A. Madoury, and D. Mailly, *Phys. Rev. B*, 1997, **55**, 3046

[9] (a) I.L. Danilovich, E.V. Karpova, I.V. Morozov, A.V. Ushakov, S.V. Streltsov, A.A. Shakin, O.S. Volkova, E.A. Zvereva, and A.N. Vasiliev, *ChemPhysChem*, 2017, **18**, 2482. (b) R.C. Alecio, J. Strecka, and M.L. Lyra, *J. Magn. Magn. Mater.*, 2018, **451**, 218. (c) H.-G. Cheng, M. Li, Y.-Y. Wu, M. Wang, D. Zhang, J. Bao, B. Guo, and Z.-Y. Sun, *Phys. Rev. A*, 2020, **101**, 052116

[10] C.P. Landee, and M.M. Turnbull , *Eur. J. Inorg. Chem.*, 2013, 2266

[11] (a) M. Chiba, T. Fukui, Y. Ajiro, M. Hagiwara, T. Goto, and T. Kubo, *Physica B*, 1998, **246–247**, 576. (b) M. Hagiwara, H. A. Katori, U. Schollwock, and H.-J. Mikeska, *Physica B*, 2000, **284-288**, 1601. (c) A. Fukaya, W. Higemoto, M. Hagiwara, and K. Nagamine, *Physica B*, 2000, **289-290**, 189

[12]J.E. Lorenzo, K. Katsumata, Y. Narumi, S. Shimomura, Y. Tanaka, M. Hagiwara, H. Mayaffre, C. Berthier, O. Piovesana, T. Ishikawa, and H. Kitamura, *Phys. Rev. B*, 2004, **69**, 220409(R)

[13](a) M. Clémancey, H. Mayaffre, C. Berthier, M. Horvatic, J.-B. Fouet, S. Miyahara, F. Mila, B. Chiari, and O. Piovesana, *Phys. Rev. Lett.*, 2006, **97**, 167204. (b) M. Clémancey, H. Mayaffre, M.-H. Julien, C. Berthier, P. Ségransan, A. Hassan, A.G.M. Jansen, I. Sheikin, B. Chiari, A. Cinti, and O. Piovesana, *J. Magn. Magn. Mater.*, 2004, **272–276** (*Part 2*), 962

[14](a) H. Otha, T. Tanaka, S. Okubo, S. Kimura, H. Kikuchi, and H. Nagaosa, *J. Phys. Soc. Jpn.*, 1999, **68**, *732*. (b) H. Ohta, Y. Oshima, T. Sakurai, S. Okubo, T. Tanaka, K. Koyama, M. Motokawa, H. Kikuchi, H. Nagasawa, and J.P. Boucher, *J. Magn. Magn. Mater.*, 2001, **226-230**, 439

[15](a) P.R. Hammar, and D. Reich, *J. Appl. Phys.*, 1996, **79**, 5392. (b) P. R. Hammar, D. H. Reich, C. Broholm, and F. Trouw, *Phys. Rev. B*, 1998, **57**, 7846

[16](a) H. Deguchi, S. Sumoto, S. Takagi, M. Mito, T. Kawae, K. Takeda, H. Nojiri, T. Sakon, and M. Motokawa, *J. Phys. Soc. Jpn.*, 1998, **67**, 3707. (b) M. Mito, H. Akama, T. Kawae, K. Takeda, H. Deguchi, and S. Takagi, *Phys. Rev. B*, 2002, **65**, 104405

[17]R. Calemczuk, J. Riera, D. Poilblanc, J.-P. Boucher, G. Chaboussant, L. P. Levy, and O. Piovesana, *Eur. Phys. J. B*, 1999, **7**, 171

[18] H. Mayaffre, M. Horvatic, C. Berthier, M.-H. Julie, P. Segransan, L. Levy, and O. Piovesana, *Phys. Rev. Lett.*, 2000, **85**, 4795

[19] K. Katsumata, *Physica Scripta*, 2005, **71**, CC7-13

[20] (a) S. Wessel and S. Haas, *Phys. Rev. B*, 2000, **62**, 316-323. (b) S. Wessel, and S. Haas, *Eur. Phys. J. B*, 2000, **16**, 393

[21]E. Orignac, R. Citro, S. Cappoli, and D. Poilblanc, *Phys Rev B*, 2007, **76**, 144422

[22]M.T. Batchelor, X.W. Guan, N. Oelkers, and Z. Tsuboi, *Adv. Phys.*, 2007, **56**, 465

[23] X. Wang, and L. Yu, *Phys. Rev. Lett.*, 2000, **84**, 5399

[24] B. Normand, J. Kyriakidis, and D. Loss, *Ann. Phys.* (Lepzig), 2000, **9**, 133

[25] C.A. Hayward, D. Poilblanc, and L.P. Levy, *Phys. Rev. B*, 1996, **54** R12 649

[26] M. Usami, and S.-I. Suga, *Phys. Rev. B*, 1998, **58**, 14401

[27] (a) Q. Gu, and J.-L. Shen, *Phys. Lett. A*, 1999, **251**, 150. (b) Q. Gu, D.-K. Yu, and J.-L. Shen, *Phys. Rev. B*, 1999, **60**, 3009

[28] W. Zheng, R.R.P. Singh, and J. Oitmaa, *Phys. Rev. B*, 1997, **55**, 8052

[29] (a) M. Hagiwara, Y. Narumi, K. Kindo, T. Nishida, M. Kaburagi, T. Tonegawa, *Physica B*, 1998, **246-247**, 234; (b) M. Hagiwara, H.A. Katori, U. Schollwöck, and H.-J. Mikeska, *Phys. Rev. B*, 2000, **62**, 1051.

[30] T. Verkholyak, and J. Strecka, *J. Phys. A: Math. Theor*., 2012, **45**, 305001

[31] (a) R. Chitra and T. Giamarchi, *Phys. Rev. B*, 1997, **55**, 5816. (b) A. Furusaki and S.-C. Zhang, *Phys. Rev. B*, 1999, **60**, 1175

[32] T. Giamarchi and A.M. Tsvelik, *Phys. Rev. B* 1999, **59**, 11398

[33] T. Nikuni, M. Oshikawa, A. Oosawa, and H. Tanaka, *Phys. Rev. Lett.* 2000, **84**, 5868.

[34] T. Hong, Y.H. Kim, C. Hotta, Y. Takano, G. Tremelling, M.M. Turnbull, C.P. Landee, H.-J. Kang, N.B. Christensen, K. Lefmann, K.P. Schmidt, G.S. Uhrig, and C. Broholm, *Phys. Rev. Lett.*, 2010, **105**, 137207

[35] (a) C. Lacroix, P. Mendels, and F. Mila (ed) *Introduction to Frustrated Magnetism (Springer Series in Solid-State Science*, vol 164), Springer, Berlin, 2011. (b) U. Schollwöck, J. Richter, D.J.J. Farnell, and R.F. Bishop (ed) *Quantum Magnetism (Lecture Notes in Physics* vol 645) Springer, Berlin, 2004.

[36] The methods used to calculate M(H) are: (1) Hatfield theory,[37,38,39] (2) from the cluster approach developed by Bonner and Fischer,[40] (3) effective field theories of magnetism,[41,42] (4) one magnon model,[4a-c,8,15b] or (5) series expansions.[28]

[37] W.E.J. Hatfield, *Appl. Phys. Rev. A*, 1981, ***52***, 1985

[38] J.W. Hall, W.E. March, R.R. Weller, and W.E. Hatfield, *Inorg. Chem*., 1981, **20**, 1033

[39] D.B. Brown, J.A. Donner, J.W. Hall, S.R. Wilson, D.J. Hodgson, and W.E. Hatfield, *Inorg. Chem*., 1979, **18**, 2635

[40] J.C. Bonner, and M.E. Fisher, *Phys. Rev. A*, 1964, **135**, 640

[41] B.E. Myers, L. Berger, and S.A. Friedberg, *J.* Appl. Phys., 1968, **40**, 1149

[42] J.S. Smart, *Effective Field Theories of magnetism*, Saunders, Philadelphia, PA, 1966

[43] The different techniques employed to calculate M(H) are: (1) Lanczos exact diagonalization using finite models with periodic boundary conditions (also referred to as repulsive boson model)[21,25], (2) dimer series expansions[5,28], (3) critical exponent calculation of the spin correlation function[26] , (4) fitting to spin ladder Hamiltonian model with Zeeman term[29a], (5) transfer-matrix renormalization group (TMRG) technique[23], (6) extensive renormalization group (RG) approach[24] , and (7) integrable ladder model based of the High Temperature Expansion method[22].

[44] M. Deumal, M.J. Bearpark, J.J. Novoa, M.A. Robb, *J. Phys. Chem. A*, 2002, **106**, 1299

[45] J. Jornet-Somoza, M. Deumal, J. Borge, M.A. Robb, *J. Phys. Chem. A*, 2018, **122**, 2168

[46] DFT/UB3LYP: (a) A.D. Becke, *Phys. Rev. A*, 1988, **38**, 3098. (b) C. Lee, W. Yang, and R.G. Parr, *Phys. Rev. B*, 1988, **37**, 785

[47] M.J. Frisch, G.W. Trucks, H.B. Schlegel, G.E. Scuseria, M.A. Robb, J.R. Cheeseman, J.A. Montgomery, Jr., T. Vreven, K.N. Kudin, J.C. Burant, J.M. Millam, S.S. Iyengar, J. Tomasi, V. Barone, B. Mennucci, M. Cossi, G. Scalmani, N. Rega, G.A. Petersson, H. Nakatsuji, M. Hada, M. Ehara, K. Toyota, R. Fukuda, J. Hasegawa, M. Ishida, T. Nakajima, Y. Honda, O. Kitao, H. Nakai, M. Klene, X. Li, J.E. Knox, H.P. Hratchian, J.B. Cross, V. Bakken, C. Adamo, J. Jaramillo, R. Gomperts, R.E. Stratmann, O. Yazyev, A.J. Austin, R. Cammi, C. Pomelli, J.W. Ochterski, P.Y. Ayala, K. Morokuma, G.A. Voth, P. Salvador, J.J. Dannenberg, V.G. Zakrzewski, S. Dapprich, A.D. Daniels, M.C. Strain, O. Farkas, D.K. Malick, A.D. Rabuck, K. Raghavachari, J.B. Foresman, J.V. Ortiz, Q. Cui, A.G. Baboul, S. Clifford, J. Cioslowski, B.B. Stefanov, G. Liu, A. Liashenko, P. Piskorz, I. Komaromi, R.L. Martin, D.J. Fox, T. Keith, M.A. Al-Laham, C.Y. Peng, A. Nanayakkara, M. Challacombe, P.M.W. Gill, B. Johnson, W. Chen, M.W. Wong, C. Gonzalez and J.A. Pople, Gaussian 03, Revision C.02, Gaussian, Inc., Wallingford CT, 2004

[48] F. Neese, ORCA - An ab Initio, Density Functional and Semiempirical Program Package, Version 3.0; Max Planck Institute for Bioinorganic Chemistry: Müllheim, 2012

[49] P.C. Harharan, and J.A. Pople, *Theor. Chim. Acta*, 1973, **28**, 213

[50] A. Shafer, H. Horn, and R.J. Ahlrich, *Chem. Phys*., 1992, **97**, 2751

[51] O. Kahn, *Molecular Magnetism*, VCH Publishers, New York, 1993 (p. 212 for same derivation applied to dinuclear compounds).

[52] (a) M. Deumal, G. Giorgi, M.A. Robb, M.M. Turnbull, C.P. Landee, and J.J. Novoa, *Eur. J. Inorg. Chem.*, 2005, 4697. (b) J. Jornet, M. Deumal, J. Ribas-Arino, M.J. Bearpark, M.A. Robb, R.G. Hicks, and J.J. Novoa, *Chem. Eur. J.*, 2006, **12**, 3995. (c) A. Shapiro, C.P. Landee, M.M. Turnbull, J. Jornet, M. Deumal, J.J. Novoa, M.A. Robb, and W. Lewis, *J. Am. Chem. Soc.*, 2007, **129**, 952. (d) L. Li, M.M. Turnbull, C.P. Landee, J. Jornet, M. Deumal, J.J. Novoa, and J.L. Wikaira, *Inorg. Chem.*, 2007, **46**, 11254. (e) J. Jornet-Somoza, M. Deumal, M.M. Turnbull, and J.J. Novoa, *Polyhedron*, 2009, **28**, 1965. (f) J. Jornet-Somoza, M. Deumal, C.P. Landee, M.M. Turnbull, and J.J. Novoa, *Inorg. Chem.*, 2010, **49**, 8017. (g) S. Vela, A. Sopena, J. Ribas-Arino, J.J. Novoa, and M. Deumal, *Chem. Eur. J.*, 2014, **20**, 7083. (h) S. Vela, M. Fumanal, and M. Deumal, *Dalton Trans.*, 2015, **44**, 608

[53] We have chosen such a limit to be |0.1| cm-1 due to the number of significant digits we have in the energy of the high and low spin states, with the cutoffs employed in the computation of the integrals and in the self-consistent process.

[54] (a) C.S. Clarke, J. Jornet, M. Deumal, and J.J. Novoa, *Polyhedron*, 2009, **28**, 1614. (b) C.S. Clarke, J. Jornet-Somoza, F. Mota, J.J. Novoa, and M. Deumal, *J. Am. Chem. Soc.*, 2010, **132**, 17817. (c) S. Vela, F. Mota, M. Deumal, R. Suizu, Y. Shuku, A. Mizuno, K. Awaga, M. Shiga, J.J. Novoa, and J. Ribas-Arino, *Nat. Commun.*, 2014, **5**, 4411. (d) S. Vela, M. Deumal, M. Shiga, J.J. Novoa, and J. Ribas-Arino, *Chem. Sci.*, 2015, **6**, 2371. (e) T. Francese, J. Ribas-Arino, J.J. Novoa, R.W.A. Havenith, C. de Graaf, and M. Deumal, *Phys. Chem. Chem. Phys.*, 2018, **20**, 20406

[55] Charge Model 5, CM5: (a) A.V. Marenich, S.V. Jerome, C.J. Cramer, and D.G. Truhlar, *J. Chem. Theory and Comput*. 2012, **8**, 527. Hirshfeld spin density: (b) F.L. Hirshfeld, *Theor. Chem. Acc.,* 1977, **44**, 129-38. (c) J. P. Ritchie and S. M. Bachrach, *J. Comp. Chem.*, 1987, **8**, 499.

[56] (a) F.M. Romero, R. Ziessel, M. Bonnet, Y. Pontillon, E. Ressouche, J. Schweizer, B. Delley, A. Grand, and C. Paulsen, *J. Am. Chem. Soc.*, 2000, **122**, 1298. (b) D. Maspoch, L. Catala, P. Gerbier, D. Ruiz-Molina, J. Vidal-Gancedo, K. Wurst, C. Rovira, and J. Veciana, *Chem. Eur. J.*, 2002, **8**, 3635. (c) J. Choi, J.D. Woodward, J.L. Musfeldt, C.P. Landee, and M.M. Turnbull, *Chem. Mater.*, 2003, **15**, 2797. (d) S. Vela, J. Jornet-Somoza, M.M. Turnbull, R. Feyerherm, J.J. Novoa, and M. Deumal, *Inorg. Chem.*, 2013, **52**, 12923